Constant surface tension simulations of lipid bilayers: The sensitivity of surface areas and compressibilities

Scott E. Feller
Department of Chemistry, Wabash College, Crawfordsville, Indiana 47933

Richard W. Pastor
Biophysics Laboratory, Center for Biologics Evaluation & Research, Food & Drug Administration, Bethesda Maryland

(Received 14 January 1999; accepted 19 April 1999)

Eight molecular dynamics simulations of a hydrated lipid bilayer have been carried out differing only in the applied surface tension, γ, defining the boundary conditions of the periodic cell. The calculated surface area per molecule and deuterium order parameter profile are found to depend strongly on γ. We present several methods to calculate the area compressibility modulus, K_A, from the simulations. Equivalence between the constant area and constant surface tension ensembles is investigated by comparing the present simulations with earlier work from our laboratories and we find simulation results to depend much more strongly on the specified surface area or surface tension than on the ensemble employed. © *1999 American Institute of Physics.* [S0021-9606(99)71327-9]

INTRODUCTION

Molecular dynamics simulation of lipid bilayer membranes is a field that has grown tremendously during the past decade.[1,2] As is common in liquid state simulations, periodic boundary conditions are generally employed. In addition to eliminating ''edge effects'' in the relatively small patches of membrane, these boundary conditions are natural because the model membranes most often studied in the laboratory are in the form of multilamellar arrays with a regular repeat spacing. Early simulations relied on experimental estimates for the dimensions of the periodic cell. The length normal to the surface was equated with the bilayer repeat spacing, D, which is directly determined from x-ray diffraction. The cell area was fixed by the number of lipid molecules and experimental estimates of the surface area per molecule, A_0, obtainable from combinations of x-ray diffraction, nuclear magnetic resonance (NMR), and gravimetric data. Over the past several years an increasing number of molecular dynamics (MD) simulations of lipid bilayers employing periodic simulation cells with flexible dimensions have been reported. In these simulations, the pressure tensor, **P**, is specified, and the size and shape of the cell adjusts to maintain the pressure along each cell dimension. In addition to being a more stringent test of potential energy parameters, these methods offer the possibility of determining membrane dimensions directly from simulation. It would be especially valuable to determine the area per molecule because, in contrast to D which can be obtained unambiguously from experiment, estimates of A_0 rely on an interpretation of experimental data and can vary by as much as 25% even for pure bilayers.[3] Membranes of heterogeneous composition, particularly those with embedded peptides or proteins, present even greater challenges.

As one would expect in a relatively new area of research, different viewpoints have appeared in the literature over the correct way to carry out constant pressure bilayer simulations. The first flexible cell simulations employed an isotropic pressure tensor, i.e., $P_{xx}=P_{yy}=P_{zz}$.[4–7] Zhang *et al.*[8] pointed out that interfacial systems, in general, require additional considerations when simulating at constant pressure due to the existence of a surface tension at the boundary between two phases. The surface tension, γ, is related to the pressure tensor by

$$\gamma=\langle L_z\times(P_{zz}-\tfrac{1}{2}P_{xx}-\tfrac{1}{2}P_{yy})\rangle,$$

where L_z and P_{zz} denote the length of the unit cell and component of the pressure tensor normal to the surface, respectively, and P_{xx} and P_{yy} are tangential components of the pressure tensor. Positive values of the surface tension result from tangential pressures that are less than the pressure along the normal. Interfacial systems may be simulated in a variety of statistical mechanical ensembles, commonly denoted by the thermodynamic variables which specify the system. For example, the canonical ensemble is often referred to as NVT for constant particle number (N), volume (V), and temperature (T). The dimensions of the unit cell do not vary over the course of simulations in this ensemble. In the NP_NAT ensemble, L_z varies to maintain a constant normal pressure (P_N) while the surface area (A) remains fixed. In both the NVT and NP_NAT ensembles the surface tension may be calculated during the simulation from evaluation of the pressure tensor because its conjugate thermodynamic variable, A, is fixed. To employ a fully flexible simulation cell, all components of the pressure tensor must be specified. Simulations employing an isotropic pressure tensor (i.e., zero surface tension) are generally described as being carried out in the NPT ensemble, while those allowing for a nonzero surface tension are in the $NP_N\gamma T$ ensemble. We will refer to both approaches as ''constant pressure molecular dynamics'' in this paper. For a more thorough discussion of the thermodynamics of interfacial systems as they relate to MD simulation, the reader is referred to Ref. 8.

Unlike P_N and T, and unfortunately for practitioners of membrane simulation, the appropriate value of γ is not directly specified by an observable macroscopic quantity. This is because direct experimental determination of the surface tension for a microscopic (i.e., simulation sized) patch of lipid bilayer is not presently possible. Theoretical arguments concerning the value of the membrane surface tension have recently been renewed. One viewpoint holds that the surface tension of a bilayer must be zero in a stress free membrane because the system is at its free energy minimum with respect to molecular surface area, $\gamma=(\partial G/\partial A)_{NTP_N}=0$.[9,10] In previous publications,[11,12] we have presented arguments for a nonzero surface tension based on the confining effects inherent in imposing periodic boundary conditions on lipid assemblies that are typically 5–10 molecular diameters in lateral dimension. Additional reasons why the surface tension in a lipid bilayer could be nonzero were presented by White.[13] More recently, Marsh[14] and Chiu *et al.*[15] (who also carried out MD simulations) explicitly argued that the expected value of γ in the present simulations should be greater than zero.

The practical effect of the choice of applied surface tension on simulations of lipid bilayers in the liquid crystal (L_α) phase has recently been studied by Tieleman and Berendsen,[16] who carried out a series of ~250 ps MD simulations at zero and nonzero (28 dyn/cm) surface tensions. They concluded that the two different surface tensions yielded no significant difference in the membrane dimensions or other structural and dynamic properties examined. They did, however, find significant differences during the course of their simulations when the water model, partial atomic charges, or Lennard-Jones parameters were altered, suggesting that simulation results are more sensitive to the potential energy function than to the value of the lateral pressure.

Our own previous simulation results for L_α phase dipalmitolyphosphatidylcholine (DPPC) bilayers do not agree with those of Tieleman and Berendsen. In preliminary work,[17] an applied surface tension of zero led to a 5% shrinkage of the surface area over the course of 50 ps. In a more recent series of four, 800 ps NP_NAT simulations,[18] calculated surface tensions only varied from 26 to 39 dyn/cm over an area range of 59 to 68 Å^2/lipid. These results imply that a 28 dyn/cm difference in γ would lead to substantial changes in A_0.

The preceding descrepency could arise from a variety of factors, including time scale, length scale, algorithms, and potential energy functions. To help clarify this matter, this paper presents results for eight, 1 nanosecond $NP_N\gamma T$ simulations on an L_α phase DPPC lipid bilayer, using a range of applied surface tensions from 0 to 55 dyn/cm. The resulting differences in surface areas per molecule and deuterium order parameter profiles are compared with available experimental data. Also considered are a number of technical issues that must be resolved in carrying out constant pressure bilayer simulations, including: time scales of area fluctuations, the evaluation of the area compressibility, and the equivalence the NP_NAT and $NP_N\gamma T$ ensembles.

PROCEDURE

The periodic simulation cell contained 72 lipid molecules (36 per monolayer) and 29.1 water molecules per lipid for a total of 15 642 atoms. This water/lipid ratio corresponds to full hydration of the bilayer. The temperature was maintained at 50 °C by means of the Hoover thermostat.[19] A fully flexible simulation cell was employed with the z dimension (i.e., the bilayer normal) adjusted to maintain the $P_{zz}=1$ atm, and the x and y dimensions varied to maintain the desired γ. A variant of the extended system formalism, the Langevin Piston algorithm,[20] was used to maintain the pressure and surface tensions at their chosen values, with piston mass of 500 amu and a collision frequency of 5 ps^{-1}. Surface tensions of 0, 35, 40, 45, 50, and 55 dyn/cm were studied, where the surface tension values are given on a per interface basis (i.e., the tension applied to the entire bilayer was twice these values). The initial area was set to 62.9 Å^2/lipid, as consistent with the recent experimental determination of Nagle and co-workers.[21] Initial coordinates were taken from the 800 ps point of the previously noted NPAT simulation.[18] For γ values of both 35 and 50 dyn/cm, a second simulation was carried out using initial conditions from the 300 ps point of the same NPAT simulation. The program CHARMM[22] (Chemistry at HARvard Molecular Mechanics) was used with the PARM22b4b all-atom parameter set.[23] The CHARMM potential contains terms for bond lengths, bond angles, torsional angles, and improper torsional angles. The interactions between nonbonded atoms are described by Coulombic interactions between partial point charges on the atomic centers and a Lennard-Jones (LJ) 6–12 potential. The LJ potential was switched smoothly to zero over the region from 10–12 Å. Electrostatic interactions were included via the particle mesh Ewald summation.[24] All bonds involving hydrogen were fixed at their equilibrium distances using the SHAKE algorithm.[25] A timestep of 2 fs was employed with a modified leap-frog Verlet integration scheme. A neighbor list, used for calculating the LJ potential and the real space portion of the Ewald sum, was kept to 14 Å and updated every 20 fs. Coordinates sets were saved every 1 ps for subsequent analysis. Simulations were carried out using either a 4-processor K420 Hewlett-Packard server (for a rate of 1.25 hr/ps) or 8 processors of an IBM SP2 (2 hr/ps). Each simulation was 1 ns in length.

RESULTS

Surface area

The instantaneous surface area per molecule is plotted in Fig. 1 for each of the simulations. Large fluctuations are observed in all cases, and substantial drift from the initial condition for some. Qualitatively, higher γ lead to larger surface areas (the bilayer is *pulled* by an applied surface tension), and $\gamma=0$ results in a dramatic contraction in the area as consistent with our earlier observations.[17] Even though the present simulations are long and computationally expensive by present standards, equilibrium has probably not been reached for all values of γ. For example, the large (and sudden) expansions for both $\gamma=50$ trajectories suggest a possible disruption of the bilayer. In contrast, the system

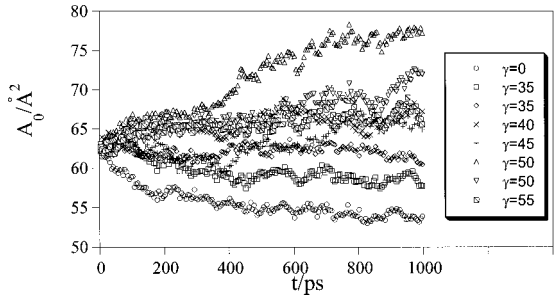

FIG. 1. Surface area per molecule as a function of time for each of the constant surface tension simulations.

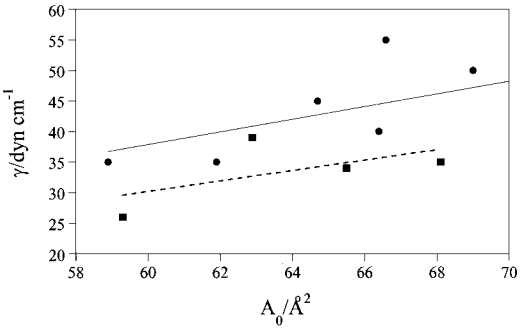

FIG. 2. Surface tension vs molecular surface area from $NP_N\gamma T$ simulations (circles) and NPAT simulations (Ref. 18) (squares). The lines give the best linear fit to the data.

remained stable at $\gamma=55$, and the surface areas are similar to those calculated for $\gamma=40$ and 45. The instantaneous surface areas for the pair of $\gamma=35$ simulations drift apart at approximately 200 ps, and do not cross again. These observations indicate that convergence of the surface area is not guaranteed on the 1 ns time scale, and that a difference of 10 dyn/cm in an applied surface tension is only marginally resolvable.

With the preceding caveats in mind, we consider averages calculated over 500–1000 ps for our primary analysis. The average area per molecule, A_0, obtained for each γ is listed in the second column of Table I. The $\gamma=0$ simulation resulted in a surface area that is much too small for a fluid phase DPPC bilayer, while both $\gamma=50$ simulations took on values that were too large. From the present simulations, it appears that surface tensions in the range 35–45 dyn/cm are needed to produce stable systems with reasonable values of the area per molecule. These results agree with our earlier predictions that the value of the applied surface tension necessary to simulate a patch of membrane this size is in the range of 30–40 dyn/cm.[11,12]

Compressibility modulus

Near the free energy minimum, the change in A_0 as a function of γ can be related to the area compressibility modulus, K_A,

$$\left(\frac{\partial\gamma}{\partial A_0}\right)_T=\frac{K_A}{A_0^*}, \tag{1}$$

TABLE I. Mean values and rms fluctuations for the area per molecule, A_0, calculated during the final 500 ps of each simulation. The values of the compressibility modulus, K_A, were calculated using Eq. (3). Experimental values of A_0 and K_A are 62.9 Å^2 and 140 dyn/cm, respectively.

γ/dyn cm^{-1}	A_0/Å^2	$\langle\delta A_0^2\rangle^{1/2}$/Å^2	K_A/dyn cm^{-1}
0	54.3	0.64	1640
35	58.9	0.71	1450
35	61.9	0.81	1170
40	66.4	1.03	780
45	64.7	1.42	400
50	75.8	1.45	450
50	69.0	1.54	360
55	66.6	0.97	880

where A_0^* is the surface area per molecule at the free energy minimum. Figure 2 plots γ vs the calculated A_0 for $\gamma>0$, and the best fit straight line. (The zero surface tension point is not included because it is clearly far from the true minimum.) Inserting the slope into Eq. (1) and setting $A_0^*=62.9\,\text{Å}^2$ leads to $K_A=130\pm60$ dyn/cm, where the standard deviation was evaluated from the regression parameters (see Ref. 26, p. 56). (Note that present surface tensions are reported on a per interface basis.) The agreement with experiment,[27] $K_A=140$ dyn/cm, is quite satisfactory given the large statistical errors in the simulation. Figure 2 also plots the calculated surface tension vs A_0 from our *constant area* MD simulations of the same system.[18] A linear fit of this data yields $K_A=107\pm104$ dyn/cm. (The larger statistical error of this estimate is consistent with the smaller amount of data.) Although the precision of our compressibility moduli is low and Eq. (1) is valid only for small changes in the surface area, these results lend support to both the equivalence of the NP_NT and NP_NAT ensembles and the ability of the current potential energy function to reproduce the elastic properties of the membrane.

The compressibility modulus can also be related to the mean squared fluctuations in membrane area

$$\langle\delta A^2\rangle=kT\left(\frac{\partial A}{\partial\gamma}\right)_T=kT\frac{A}{K_A}, \tag{2}$$

where A is the total area of the membrane. Equation (2) can be rewritten in terms of fluctuation in the area per molecule and rearranged to yield an expression for the compressibility modulus

$$K_A=\frac{kTA_0}{N\langle\delta A_0^2\rangle}. \tag{3}$$

The third and fourth columns of Table I contain the root-mean-squared (rms) fluctuations in A_0 and the corresponding compressibility moduli calculated from Eq. (3). All of these calculated K_A are substantially larger than were obtained from the slope of γ vs A_0 (Fig. 2), with an average $\pm$ standard error of 780 ± 160 dyn/cm for simulations carried out with $\gamma>0$.

Errors in $\langle \delta A^2 \rangle$

The preceding values of K_A, too high by a factor of four, imply that the fluctuations in surface area observed in the simulation are too small by a factor of two; i.e., inserting the experimental value $K_A = 140$ dyn/cm into Eq. (3) leads to $\langle \delta A^2 \rangle = 2.4\,\text{Å}^4$. The discrepancy could result from a variety of causes, including: (i) deficiencies in the potential energy function; (ii) small system size; (iii) insufficient sampling of lower frequency modes. The values of K_A obtained from slope of γ vs A_0 [Eq. (1)] indicate that the potential energy function is reasonable, though molecular mechanics force fields can model some properties better than others. Imposing periodic boundary conditions on a small system (only 36 lipids per side) eliminates most membrane undulations,[11] and expansions and contractions of the surface area could also be inhibited. For example, some components of stretching might involve motions of larger clusters of lipids, or are coupled with lower wavelength undulations. Before pursuing these possibilities, however, it is important to eliminate statistical errors. The remainder of this subsection considers this issue.

Insufficient sampling can lead to unacceptably large variability in an estimated mean, or actual bias. The first point to make regarding the variability is that statistical errors are expected to be greater in the fluctuations of means than of the means themselves. Specifically, for a simulation of length T_{run} the variance $\sigma^2[A]$ of the area is given by[28]

$$\sigma^2[A] = (2\tau/T_{\text{run}})\langle \delta A^2 \rangle, \tag{4}$$

where τ is the relaxation time of the correlation function

$$C(t) = \langle \delta A(0)\, \delta A(t) \rangle, \tag{5}$$

and T_{run} is assumed to be much greater than τ. If the process is Gaussian and $C(t)$ is single exponential, the variance in the fluctuation is[28]

$$\sigma^2[\delta A^2] = (2\tau/T_{\text{run}})\langle \delta A^2 \rangle^2. \tag{6}$$

Hence, other things being equal, it is expected that an estimate of K_A from the area would be more precise than one from its fluctuations.

Figure 3(a) shows the correlation function defined by Eq. (5) calculated for each trajectory. The large variability is consistent with trajectory lengths of less than 10 times the correlation time. To obtain a more precise estimate of τ, we assume the differences among the correlation functions at different γ are due solely to random sampling error, and average to obtain a single correlation function, $\overline{C}(t)$ [Fig. 3(b) symbols]. Fitting $\overline{C}(t)$ to an exponential decay function [Fig. 3(b), solid line] results in a correlation time, τ, of ~50 ps. Using the formula of Zwanzig and Ailawadi,[29] we can estimate the standard deviation in $\overline{C}(t)$

$$\sigma[\overline{C}(t)] = \left(\frac{2\tau}{T_{\text{run}}}\right)^{1/2} \times (1 - \overline{C}(t)). \tag{7}$$

Figure 3(b) plots $\overline{C}(t) \pm \sigma[\overline{C}(t)]$, using both the standard deviation calculated from the set of simulations (solid squares) and the values given by Eq. (7) (dashed line), showing that the distribution of correlation times observed in the simulation is consistent with a correlation time of 50 ps common to all γ values.

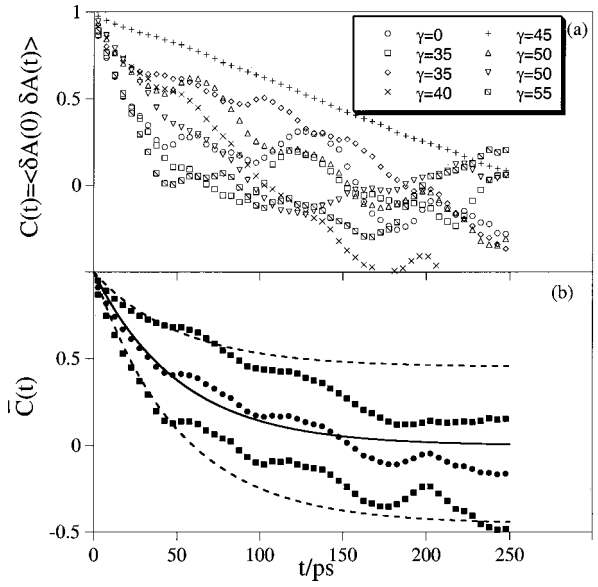

FIG. 3. Autocorrelation function, $C(t) = \langle \delta A(0)\, \delta A(t) \rangle$, (a) from the final 500 ps of the eight simulations, i.e., the correlation functions are calculated to 1/2 the run time, (b) using data averaged over all eight simulations. The circles show the mean correlation function with the squares representing ± one standard deviation as calculated from the eight simulations. The solid line gives a best fit of the average correlation function to an exponential, and the dashed lines give ± one standard deviation as estimated from Eq. (4).

Using the values $\tau = 50$ ps, $T_{\text{run}} = 500$ ps, and $\langle \delta A^2 \rangle = 2.4\,\text{Å}^4$ (consistent with the experimental K_A), we estimate $\sigma[A] = 1.1\,\text{Å}^2$ and $\sigma[\delta A^2] = 2.5\,\text{Å}^4$ from Eqs. (4) and (5), respectively. Given that the large variance observed in the correlation functions at long times makes it difficult to quantify the time scale of fluctuations occurring over periods greater than 50 ps (but certainly does not preclude their existence), the preceding estimates of the statistical errors should be considered lower limits. The large statistical error in the fluctuations (larger than the values themselves) indicates severe undersampling. Such undersampling can lead to systematic underestimates of quantities such as fluctuations. Differences in the time averaged areas for the pairs of simulations at $\gamma = 35$ and 50 dyn/cm (Table I) suggest that longer simulations would lead to area fluctuations of larger magnitude. Combining the area values observed in the pair of $\gamma = 35$ dyn/cm simulations, for example, gives $\sigma_{A0} = 1.7\,\text{Å}^2$ and $K_A = 258$ dyn/cm. On this basis, we conclude that the large errors in K_A estimated from the fluctuations are most likely associated with high statistical error. The A_0 for the $\gamma = 35$ simulations are well within 2σ (i.e., 2.2 Å^2) of their mean, indicating that undersampling in the calculation of means is not as severe as for the fluctuations.

Deuterium order parameters

We now turn to analysis of single molecule properties that characterize the structure and dynamics of the phospholipid bilayers. A particularly useful quantity describing the structure of the alkyl chains is the deuterium order parameter,

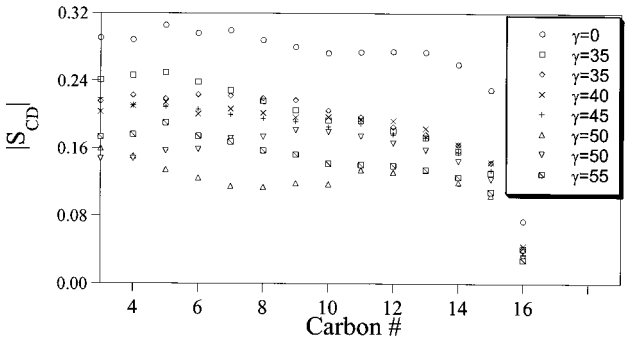

FIG. 4. The deuterium order parameter profile calculated from the constant surface tension simulations.

$$S_{CD}=\langle \tfrac{3}{2}\cos^2\theta-\tfrac{1}{2}\rangle, \tag{8}$$

where θ is the angle between the CH bond vector and the bilayer normal. Figure 4 shows the deuterium order parameter profile for each of the simulations. All simulations produce order parameter profiles with the general features observed experimentally[30,31] for DPPC at 50 °C (a plateau region near the carbonyls with $|S_{CD}|\cong 0.20-0.22$, followed by a decrease in order to near zero at the terminal methyl), with the best agreement obtained for γ between 35 and 45. Runs employing $\gamma=0$ or $\gamma\geqslant 50$ produced profiles that were unrealistically high and low, respectively, consistent with the average surface areas observed in those simulations.

Lateral displacements and density fluctuations

The freedom of the x and y elements of the unit cell to vary during the course of the $NP_N\gamma T$ simulations would seem to enhance surface density fluctuations among the lipids in the membrane, possibly influencing the rate of lateral displacement. Diffusion is a very slow process on the MD time scale, however, so that effects on the simulation arising from different ensembles may be negligible. To investigate this effect, the center-of-mass lateral displacement correlation function

$$L(t)=\langle (x(t)-x(0))^2+(y(t)-y(0))^2\rangle, \tag{9}$$

has been calculated from each of the $NP_N\gamma T$ simulations and plotted in Fig. 5(a). In Eq. (9) the brackets denote an averaging over 500 ps in time and over 72 lipid molecules. On this time scale, $L(t)$ yields information on fast displacements (''rattling in a cage'') and, to a lesser extent, rotational relaxation of the whole molecule (or ''wobble''), but not translational diffusion involving exchange of lipids.[32] The correlation functions show statistical variation but no systematic trend (e.g., more rapid diffusion as the surface area increases). The weak dependence of diffusion rate on surface area is also seen when $L(t)$ is calculated from the trajectory of the constant area simulations [Fig. 5(b)], and provides further support for the equivalence of the $NP_N\gamma T$ and NP_NAT ensembles. This finding does not necessarily rule out surface density fluctuations playing a role in translational motion as it is possible that the density fluctuations on a smaller scale, i.e., individual molecules, are more important than fluctuations involving the patch of membrane being

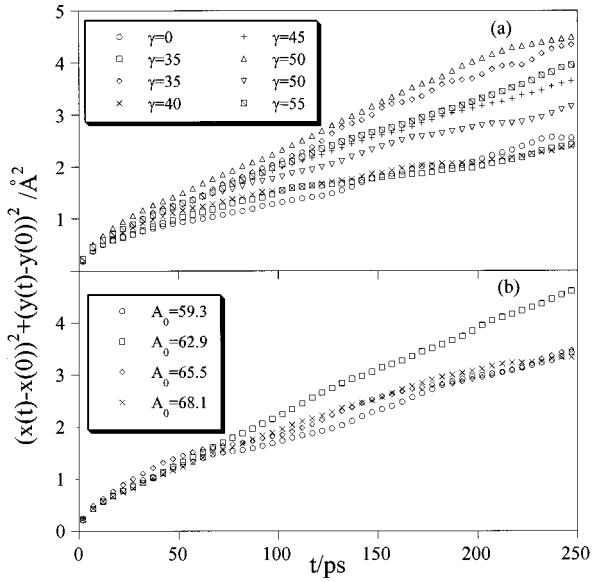

FIG. 5. The lateral displacement correlation function calculated from (a) constant surface tension simulations, and (b) constant surface area simulations.

simulated. It is also possible that on a longer time scale differences between ensembles will be observed as molecules, or clusters of molecules, undergo true diffusion (as opposed to rattling).

The evaluation of lateral density fluctuations at the level of single molecules requires a method to define individual molecular areas. Shinoda and Okazaki recently proposed the use of Voronoi polyhedra constructed from the x and y coordinates of the lipid centers-of-mass for this purpose.[33] This method yields the time-dependent area per molecule, as well as the instantaneous number of nearest-neighbors. Typical probability distributions for the single molecule areas, calculated using the Voronoi analysis algorithm provided in Ref. 28, are plotted in Fig. 6 in solid lines. The upper panel shows $\gamma=35$ for $NP_N\gamma T$, and the lower $A_0=62.9$ for NP_NAT; this pair of simulations had the closest values of the mean molecular area, and the area/molecule agreeing best with experiment. The distributions are approximately Gaussian, with some skew toward large molecular areas, i.e., the median of the distribution is less than the mean. Average areas per lipid, fluctuations, and compressibility moduli [from Eq. (2)] are listed in Table II. Averaging over all the $NP_N\gamma T$ simulations, $K_A=235\pm 30$ dyn/cm (excluding the $\gamma=0$, $K_A=210\pm 10$ dyn/cm); the mean K_A is 255 ± 10 for the NP_NAT simulations. These overestimate experiment ($\sim$140 dyn/cm), but are significantly smaller than the values reported in Table I based on fluctuations of the entire membrane. The magnitudes of area fluctuations from the two ensembles are statistically equivalent at the 95% confidence level.

An alternative definition of single molecule areas can be obtained from a formula proposed by Nagle,[3] relating the area per molecule to the average value of the deuterium order parameter at the top of the acyl chains,

$$A_0=\frac{2\times V_{CH_2}}{(|\langle S_{CD}^{\text{plateau}}\rangle|+\tfrac{1}{2})\times 1.27}, \tag{10}$$

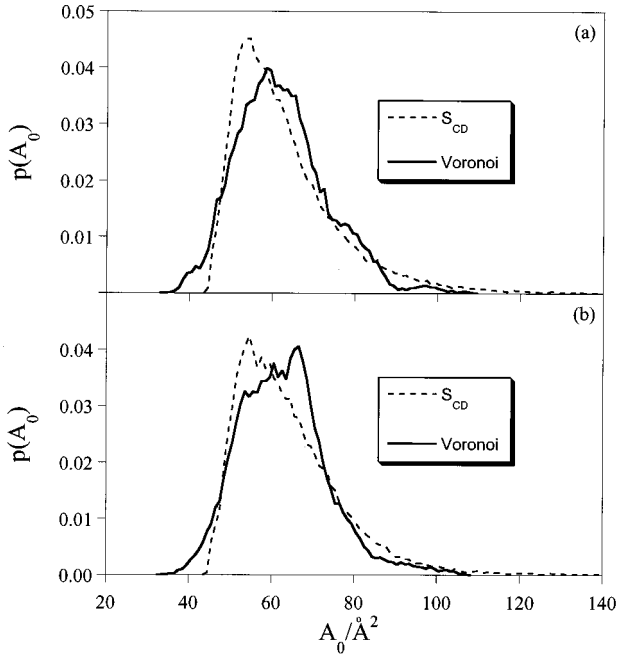

FIG. 6. Probability distributions of single molecule areas observed in (a) $NP_N\gamma T$ with $\gamma=35$ and (b) NP_NAT with $A=62.9$ simulations. Solid lines show the values obtained from Voronoi analysis and dashed lines give the values calculated from S_{CD} values using Eq. (10).

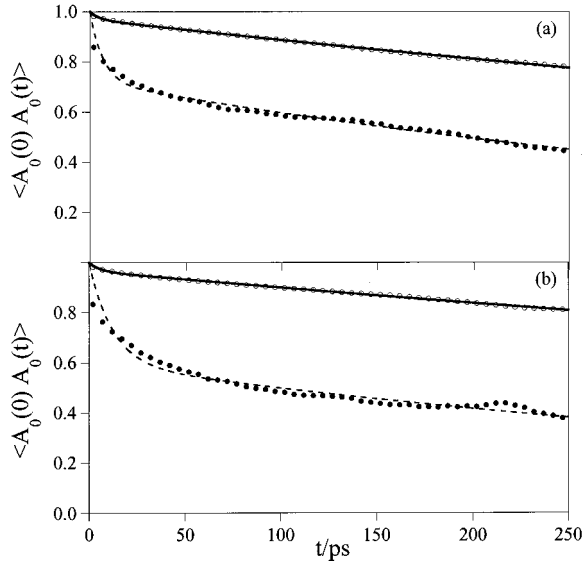

FIG. 7. Single molecular area autocorrelation function, $c(t)=\langle \delta A_0(0)\,\delta A_0(t)\rangle$, for (a) the $\gamma=35$ and (b) the $A=62.9$ simulations. The symbols represent the values of the correlation function and the lines gives the best fit of the data to a sum of two exponentials. Open symbols and solid lines were from areas calculated by Voronoi analysis while closed symbols and dashed lines were calculated from areas defined by Eq. (10).

where we have chosen to calculate the plateau region between carbons 4 and 8. For each lipid molecule an instantaneous area was determined using Eq. (10), and the results are compared with the Voronoi analysis in Fig. 6 (dashed lines) and Table II. The compressibility moduli are in very good agreement with experiment, and with the results where K_A was determined from Eq. (1). Again, no significant difference is observed between the constant tension and constant area ensembles.

The similarities between Figs. 6(a) and 6(b) suggest that unit cell flexibility has little or no effect on the fluctuations of individual molecules for the present-sized system. Although correlation of density fluctuations of single molecules and the unit cell might be possible for smaller systems, the present results again suggest no difference between the constant pressure and constant area algorithms.

The determination of single molecular area time series from Voronoi analysis or deuterium order parameters allows for the calculation of the autocorrelation function for single molecule area fluctuations, as was done for the unit cell area fluctuations (Fig. 3). The single molecule correlation functions, however, have the benefit of being averaged over 72 lipids so that their precision is much improved. Figure 7 shows $\langle \delta A_0(0)\,\delta A_0(t)\rangle_{\text{lipid}}$ for the $\gamma=35$ [Fig. 7(a)] and $A_0=62.9$ [Fig. 7(b)] simulations using instantaneous molecular

TABLE II. Single molecule area fluctuation parameters.

	Voronoi			Eq. (10)		
Simulation	$\langle A_0\rangle$/Å^2	$\langle \delta A_0^2\rangle^{1/2}$/Å^2	K_A/dyn cm^{-1}	$\langle A_0\rangle$/Å^2	$\langle \delta A_0^2\rangle^{1/2}$/Å^2	K_A/dyn cm^{-1}
$\gamma=0$	54.35	7.75	404	57.22	9.78	267
$\gamma=35$	60.17	9.95	271	62.80	13.74	148
$\gamma=35$	62.15	10.98	230	63.04	13.17	162
$\gamma=40$	66.38	11.29	232	66.59	19.10	81
$\gamma=45$	64.69	11.90	203	66.07	16.13	113
$\gamma=50$	75.77	17.38	112	73.20	17.31	109
$\gamma=50$	69.03	12.73	190	69.68	19.42	82
$\gamma=55$	66.57	11.27	234	69.00	18.23	93
Ave.			235			132
Std. dev.			83			62
$A=59.3$		10.3	251	60.20	14.73	124
$A=62.9$		10.7	242	64.36	13.78	151
$A=65.5$		11.0	243	66.19	13.86	154
$A=68.1$		10.4	283	66.18	13.32	111
Ave.			255			135
Std. dev.			19			21

areas calculated from Voronoi analysis and from Eq. (10). The long-time decay rates of all the correlation functions are approximately equal with differences between the two methods of area calculation much larger than the differences between the $NP_N\gamma T$ and NP_NAT simulations. Fitting each correlation function to a sum of 2 exponentials showed a rapid decay ($\tau_{fast} \cong 5-10$ ps) followed by a much slower relaxation ($\tau_{slow} \cong 500-1000$ ps). The rearrangements occurring on the 0.5–1 ns time scale may be due to the ''wobbling'' of the long axis of the lipid molecules, previously identified to occur on the nanosecond time scale.[32]

CONCLUSIONS

Assuming the true value of A_0 for fully hydrated, fluid phase DPPC is 62.9 Å^2, the value determined experimentally by Nagle and co-workers and strongly supported by our earlier constant area simulations, we conclude that the correct surface tension to apply is in the range 35–45 dyn/cm. The relatively large difference between the duplicate $\gamma=35$ simulations and the relatively small difference between $\gamma=40$ and 45 demonstrate the difficulty in determining this quantity to a high precision. Additionally, inaccuracies in the potential energy parameters employed could significantly alter this value. It appears, based on Figs. 3 and 7, that the inherently slow process of area fluctuation requires simulations of close to 10 ns, rather than 1 ns, before convergence and/or the generation of sufficient equilibrium sampling is obtained. Advancements in computer hardware (e.g., processor speeds) and software (e.g., parallelization tools and multiple time step algorithms) will enable routine generation of such trajectories in the near future.

Three approaches were investigated for the calculation of the bilayer compressibility modulus, K_A. Direct calculation of $d\gamma/dA$ (Fig. 2) gave values in good agreement with experiment, while the calculations based on the magnitude of membrane area fluctuations (Table I) gave K_A values as much as an order-of-magnitude too large. The latter determination, however, likely suffered from poor sampling due to the long time scale of area fluctuations. The third approach examined, determination of *single molecule* area fluctuations, shows great promise for determination of lateral compressibility because it is based on an average both over time and over the individual lipids making up the membrane. Defining the area by Voronoi polygons resulted in a K_A value that was approximately 100 dyn/cm too large while the use of deuterium order parameters gave larger area fluctuations and compressibility moduli very close to experiment. Further study of methods for the determination of single molecule areas and compressibilities could be useful for the interpretation of recent experiments suggesting that mixed chain lipids can be characterized by separate ''chain compressibilities.''[34]

Comparisons of constant area and constant surface tension simulations show no significant difference in either equilibrium or dynamic single molecule properties (S_{CD} in Fig. 4, lateral diffusion in Fig. 5, area fluctuation magnitude in Fig. 6, area fluctuation decay rate in Fig. 7) or bilayer elasticity (Fig. 2). The single molecule properties, however, were sensitive to the surface area per molecule, validating our recent constant area study. Thus, in contrast to the findings of Tieleman and Berendsen,[16] we find the simulation results to be strongly dependent on the choice of applied surface tension. The results presented here suggest the disagreement may be due to the significant differences in simulation lengths.

ACKNOWLEDGMENTS

This work was supported in part by the Phillips Laboratory, Air Force Material Command, United States Air Force, through the use of the IBM SP2 at the Maui High Performance Computing Center. S.E.F. thanks the National Science Foundation for support through Grant MCB-9728206.

[1] R. W. Pastor, Curr. Opin. Struct. Biol. **4**, 486 (1994).
[2] D. J. Tobias, K. Tu, and M. L. Klein, Curr. Opin. Colloid Interface Sci. **2**, 115 (1997).
[3] J. F. Nagle, Biophys. J. **64**, 1476 (1993).
[4] E. Egberts and H. J. Berendsen, J. Chem. Phys. **89**, 3718 (1988).
[5] W. Shinoda, T. Fukada, S. Okazaki, and I. Okada, Chem. Phys. Lett. **232**, 308 (1995).
[6] P. Huang, J. J. Perez, and G. H. Loew, J. Biomol. Struct. Dyn. **11**, 927 (1994).
[7] K. Tu, D. J. Tobias, and M. L. Klein, Biophys. J. **69**, 2558 (1995).
[8] Y. Zhang, S. E. Feller, B. R. Brooks, and R. W. Pastor, J. Chem. Phys. **103**, 10252 (1995).
[9] F. Jahnig, Biophys. J. **71**, 1348 (1996).
[10] K. Tu, D. J. Tobias, J. K. Blasie, and M. L. Klein, Biophys. J. **70**, 595 (1996).
[11] S. E. Feller and R. W. Pastor, Biophys. J. **71**, 1350 (1996).
[12] S. E. Feller and R. W. Pastor, in *Proceedings of the Pacific Symposium on Biocomputing*, edited by R. B. Altman, A. K. Dunker, L. Hunter, and T. E. Klein (World Scientific, Singapore, 1997), pp. 142–150.
[13] S. H. White, Proc. Natl. Acad. Sci. USA **77**, 4048 (1980).
[14] D. Marsh, Biophys. J. **73**, 865 (1997).
[15] S. W. Chiu, M. Clark, V. Balaji, H. L. Scott, and E. Jakobssen, Biophys. J. **69**, 1230 (1995).
[16] D. P. Tieleman and H. J. C. Berendsen, J. Chem. Phys. **105**, 4871 (1996).
[17] S. E. Feller, Y. Zhang, and R. W. Pastor, J. Chem. Phys. **103**, 10267 (1995).
[18] S. E. Feller, R. M. Venable, and R. W. Pastor, Langmuir **13**, 6555 (1997).
[19] W. G. Hoover, Phys. Rev. A **31**, 1695 (1985).
[20] S. E. Feller, Y. Zhang, R. W. Pastor, and B. R. Brooks, J. Chem. Phys. **103**, 4613 (1995).
[21] J. R. Nagle, R. Zhang, S. Tristram-Nagle, W. Sun, H. Petrache, and R. M. Suter, Biophys. J. **70**, 1419 (1996).
[22] B. R. Brooks, R. E. Bruccoleri, B. D. Olafson, D. J. States, S. Swaminathan, and M. Karplus, J. Comput. Chem. **4**, 187 (1983).
[23] M. Schlenkrich, J. Brickman, A. D. MacKerell, and M. Karplus, in *Biological Membranes: A Molecular Perspective from Computation and Experiment*, edited by K. Merz and B. Roux, (Birkhauser, Boston, 1996), pp. 31–81.
[24] U. Essman, L. Perera, M. L. Berkowitz, T. Darden, H. Lee, and L. G. Pedersen, J. Chem. Phys. **103**, 8577 (1995).
[25] J. P. Ryckaert, C. Cicotti, and H. J. C. Berendsen, J. Comput. Chem. **23**, 327 (1977).
[26] W. H. Press, S. A. Teukolsky, W. T. Vettering, and B. P. Flannery, *Numerical Recipes* (Cambridge University, New York, 1992).
[27] E. Evans and W. Rawicz, Phys. Rev. Lett. **64**, 2094 (1990).
[28] M. P. Allen and D. J. Tildesley, *Computer Simulation of Liquids* (Clarendon, Oxford, 1987).
[29] R. Zwanzig and N. K. Ailawadi, Phys. Rev. **182**, 280 (1969).
[30] A. Seelig and J. Seelig, Biochemistry **13**, 4839 (1974).
[31] J. P. Douliez, A. Leonard, E. J. Dufourc, Biophys. J. **68**, 1727 (1995).
[32] R. W. Pastor and S. E. Feller, in *Biological Membranes: A Molecular Perspective from Computation and Experiment*, edited by K. Merz and B. Roux, (Birkhauser, Boston, 1996), pp. 3–29.
[33] W. Shinoda and S. Okazaki, J. Chem. Phys. **109**, 1517 (1998).
[34] B. W. Koenig, H. H. Strey, and K. Gawrisch, Biophys. J. **73**, 1954 (1997).